adsorption of natural organic matter (NOM) is particularly slow, and the amount adsorbed during a normal contact time is far below the equilibrium adsorption capacity of PAC. Efforts have been undertaken to increase the adsorption rate and thus reduce the non-utilized PAC adsorption capacity. Reducing the PAC particle size is a potential strategy for overcoming the problem of slow adsorption because smaller PAC particles show faster adsorption kinetics than larger PAC particles (Weber et al., 1983; Najm et al., 1990). However, this strategy has not been studied except by our research group, partly because no practical technology existed for producing extremely small carbon particles and because the removal of such small particles during standard solid–liquid separation processes (coagulation, sedimentation, and rapid sand filtration) may be more difficult than the removal of conventional PAC particles. Even conventional PAC particles, probably a small size fraction, can leak into the filtrate during rapid sand filtration; such leakage has led to complaints from customers about dirty water. However, the use of a membrane-filtration process would permit the use of fine PAC with particle sizes similar to the membrane cut-off pore size.

We produced what we call super-powdered activated carbon or submicron PAC (S-PAC), which has much smaller particle size than commercially available PAC (Matsui et al., 2005, 2007, 2009), and we studied its adsorption characteristics (Matsui et al., 2004). Although S-PAC and PAC have the same isotherm adsorption capacities for phenol, the adsorption capacity of S-PAC for NOM is higher than that of PAC. We attributed the NOM adsorption capacity increase partially to the relatively higher mesopore volume of S-PAC, but the mesopore volume increase was too small to fully explain the increased NOM adsorption capacity. We used a wood-based activated carbon in our previous research, but activated carbon derived from other materials has not been yet tested to confirm the phenomenon.

Because providing a full explanation for the increased adsorption capacity of S-PAC is important for the future application of S-PAC in water/wastewater treatment, the objectives of the present study were to confirm the higher adsorption capacity of S-PAC and to clarify the mechanism of the adsorption capacity increase. In this study, we used NOM from various sources, along with polystyrene sulfonates (PSSs) and polyethylene glycols (PEGs) as model substances with known molecular weights (MWs) (Chin and Gschwend, 1991; Kilduff et al., 1996a; Karanfil et al., 1996a, 1996b; Li et al., 2003a, 2003b; Chang et al., 2004). S-PACs and PACs derived from wood, coconut shells, and coal were tested. On the basis of the results of these tests, we discuss the mechanism of NOM adsorption on activated carbon.

2. Materials and methods

2.1. Adsorbates and water samples

The characteristics of the adsorbates and water samples are listed in Table 1. SNOM, SFA, and SHA waters were prepared by dissolving Suwannee River NOM, humic acid, and fulvic acid, respectively, in ultrapure water (Milli-Q Advantage, Millipore Co.) containing inorganic ions added to make the ionic composition equal to that of water from Lake Hakucho, Hokkaido, Japan (see Table 2). SNOM was also dissolved in three ionic solutions (see Table 1): one containing Na^+, one containing $K^+ + Na^+$, and one containing $Ca^{2+} + Na^+$, designated as Solution-Na, Solution-K, and Solution-Ca, respectively. These solutions were used to examine the effect of cation types.

The PSSs were dissolved in ultrapure water containing inorganic ions added to make the ionic composition equal to that of water from Takkobu Lake (Hokkaido, Japan), for which the NOM adsorption capacities of S-PAC and PAC have been studied (Matsui et al., 2004). The PEGs were dissolved in ultrapure water brought to an alkalinity of 20 mg/L with $NaHCO_3$. All the water samples were adjusted to pH 7.0 ± 0.1 with HCl or NaOH as required and then filtered through a 0.45- or 0.2-μm polytetrafluoroethylene (PTFE) membrane filter before the batch adsorption tests. NOM concentrations were measured as dissolved organic carbon (DOC) (Sievers 900, GE Analytical Instruments) as indicated by UV absorbance at a wavelength of 260 nm (UV260, UV-1700, Shimadzu Co.). PSS concentrations were determined from the UV absorbance at 262 nm with a calibration curve. PEG concentrations were determined as DOC with a calibration curve (97–100% of carbon in PEG was measured as DOC). The ionic compositions of water samples were analyzed by ion chromatography (ICS-1000 Ion Chromatography System, Dionex).

The MW distributions of NOM contained in samples of Chibaberi water, Hakucho water, Inba water, post-coagulation water, SNOM water, SHA water, and SFA water were determined by liquid chromatography with organic carbon detection [HP1100 (Agilent Technologies, Inc.); packed column: GL-P252 (Hitachi); eluent: 0.02 M Na_2HPO_4 + 0.02 M KH_2PO_4]. PSS (MW 1800, 4600, and 6500) was used for calibration. The UV absorbance at 260 nm and the DOC (Model 810 Turbo, GE Analytical Instruments) of the column effluent were measured continuously.

2.2. Activated carbon

Commercially available wood-based PAC (Taikou-W, Futamura Chemical Industries Co., Gifu, Japan) was prepared as slurry in ultrapure water and pulverized to super-fine particles with a wet bead mill from Metawater Co. (Tokyo, Japan). In this paper, we refer to this pulverized activated carbon as S-PAC-T and the as-received PAC as PAC-T. Although S-PAC-T and PAC-T were the main types of activated carbon used in this study, we also used two other wood-based PACs (6MD, Calgon Mitsubishi Chemical Co., Tokyo, Japan; Picahydro MP 23, Veolia Water Solutions & Technologies, Singapore), two coconut-based PACs (F-100D, Calgon Mitsubishi Chemical Co.; Picahydro SP 23, Veolia Water Solutions & Technologies), and a coal-based PAC (6D, Calgon Mitsubishi Chemical Co.). These are referred as PAC-W, PAC-M, PAC-F, PAC-S, and PAC-D, respectively. S-PACs produced from these PACs are referred as S-PAC-W, S-PAC-M, S-PAC-F, S-PAC-S, and S-PAC-D, respectively. The S-PACs and PACs were stored as slurries in ultrapure water at 4 °C and used after dilution and placement under vacuum.

Table 1 – Water samples and adsorbate concentrations.

Designation	Source	Adsorbate initial concentration in experiments	Specific UV absorbance
Chibaberi water	Chibaberi River, Hokkaido, Japan (sampled on 13 Aug. 2008)	3.3 mg-DOC/L	3.2 L m^{-1} mg^{-1}
Hakucho water	Lake Hakucho, Hokkaido, Japan (sampled on 7 Nov. 2007)	2.0 mg-DOC/L	2.1 L m^{-1} mg^{-1}
Inba water	Lake Inba, Chiba, Japan (sampled on 14 Sep. 2008)	2.8 mg-DOC/L	2.2 L m^{-1} mg^{-1}
Post-coagulation water	Retentate of nano-filtration after ferric coagulation, sedimentation, and microfiltration of Arakawa River water, Saitama, Japan (Tanaka et al., 2008, sampled on 17 Feb. 2008)	5.7 mg-DOC/L	1.9 L m^{-1} mg^{-1}
SNOM water	Suwannee River NOM International Humic Substances Society, St. Paul, MN, USA	2.0 mg-DOC/L	4.1 L m^{-1} mg^{-1}
SHA water	Suwannee River Humic Acid Standard II International Humic Substances Society, St. Paul, MN, USA	2.2 mg-DOC/L	6.0 L m^{-1} mg^{-1}
SFA water	Suwannee River Fulvic Acid Standard II International Humic Substances Society, St. Paul, MN, USA	2.6 mg-DOC/L	3.9 L m^{-1} mg^{-1}
PSS-4600 water	PSS MW 4.6 kDa Polysciences Inc., Warrington, PA, USA	5.4 mg/L	
PSS-1800 water	PSS MW 1.8 kDa Polysciences Inc., Warrington, PA, USA	5.1 mg/L	
PSS-1100 water	PSS MW 1.1 k Da Polymer Standards Service, Mainz, RLP. Germany	4.8 mg/L	
PEG-8000 water	PEG MW 8.0 kDa, Wako Pure Chemical Industries, Osaka, Japan	5.0 mg/L	
PEG-3000 water	PEG of MW 3.0 kDa, Wako Pure Chemical Industries, Osaka, Japan	5.0 mg/L	
PEG-1500 water	PEG of MW 1.5 kDa, Wako Pure Chemical Industries, Osaka, Japan	5.0 mg/L	
PEG-300 water	PEG of MW 0.3 kDa, Wako Pure Chemical Industries, Osaka, Japan	5.0 mg/L	

A scanning electron microscope (SEM, JSM-7400F, Jeol, Tokyo, Japan) was used for acquiring images of S-PAC and PAC particles and for confirming the particle sizes. The particle size distributions of the S-PACs and PACs were determined by a laser light–scattering diffraction method after the addition of a mild detergent as a dispersing agent (S-PAC-T and PAC-T: LA-700, Horiba, Kyoto, Japan; the other carbons types: LMS-300, Seishin Enterprise Co., Tokyo, Japan). The pore size distributions of the PAC and S-PAC particles were measured by means of nitrogen gas adsorption. Isotherm data for nitrogen gas desorption at 77.4 K were analyzed by means of the Dollimore–Heal (DH) method to obtain the pore size distribution mainly in the mesopore region and by means of a density functional theory (DFT) method to obtain the distribution in the micropore region (Autosorb 6-AG, Autosorb for Windows for AS-3 and AS-6, Yuasa-Ionics Co., Osaka, Japan; Quantachrome Co., Boynton Beach, FL, USA). Zeta potentials of the S-PACs were determined by using a Zetasizer Nano ZS (Malvern Instruments Ltd., Malvern, UK); the PAC particles were too large for zeta potential measurement.

2.3. *Batch equilibrium adsorption tests*

S-PAC and PAC slurries were diluted, placed under vacuum, and added to 300-mL solutions containing adsorbate with mixing. Aliquots (100 mL) were transferred from the 300-mL solutions to 125-mL vials, which were agitated on a shaker for long-term mixing at a constant temperature of 20 °C. Control tests were also conducted by using multiple bottles that did not contain carbon to confirm that concentration changes during long-term mixing were negligible. Vials containing NOM and PSS were shaken for 3 and 4 weeks, respectively, those containing PEG-3.0 and PEG-8.0 were shaken for 5 days, those containing PEG-1.5 were shaken for 3 days, and those containing PEG-0.3 were shaken for 1 day. The liquid-phase adsorbate concentrations were measured after the water samples were filtered through a 0.2-μm PTFE membrane filter.

3. Results and discussion

3.1. *Particle size distributions*

PAC-T had a volumetric median particle diameter of 11.8 μm, and few particles with diameters less than 1 μm were present (the particle size distributions of PAC-T and S-PAC-T samples are shown in Fig. 1S in the supplementary information). In contrast, 73% of the S-PAC-T particles had diameters less than 1 μm, and the volumetric median diameter was 0.73 μm. The effective diameter (10% undersize) of S-PAC-T was 0.27 μm, and this value was less than 1/10 the value for PAC-T (3.9 μm).

Table 2 – Ion concentrations in water samples (mmol/L) and conductivity (μ S/cm).

	Na^+	K^+	Ca^{2+}	Mg^{2+}	Cl^-	$SO4^{2-}$	HCO_3^-	NO_3^-	Conductivity
Chibaberi water	0.36	0.06	0.23	0.26	0.27	0.17	0.52	0.00	190
Hakucho, SNOM, SHA, and SFA waters	0.34	0.21	0.07	0.03	0.26	0.04	0.17	0.02	77–89
Inba water	0.54	0.09	0.57	0.27	0.49	0.26	0.57	0.11	237
Post-coagulation water	2.61	0.25	3.89	1.56	2.91	4.34	1.90	0.27	1213
PSS waters	0.63	0.04	0.12	0.07	0.82	0.03	0.34	0.01	140
PEG waters	0.07	0	0	0	0.26	0	0.20	0	39
Solution-Na	0.89	0	0	0	0.44	0	0.37	0	97
Solution-K	0.39	0.49	0	0	0.43	0	0.37	0	97
Solution-Ca	0.38	0	0.24	0	0.43	0	0.37	0	97

Median and effective diameters of the carbon samples tested are shown in Table 3.

The changes in size before and after pulverization were confirmed visually by SEM. Fig. 2S (supplementary information) shows 2000× and 30,000× magnification images for PAC-T and S-PAC-T. The 2000× magnification image confirmed that PAC-T comprised particles with diameters from several tens of micrometers to 1 μm, whereas there were no particles with diameters of a few micrometers or larger present in S-PAC-T. The 30,000× magnification image confirmed that S-PAC-T was actually comprised of particles with diameters of less than a few micrometers. PAC-T had both relatively smooth and rough surfaces as indicated by the 30,000× magnification image. S-PAC-T also exhibited such surfaces. Pores with diameters larger than about 50 nm (macropores) were scattered at intervals on the surfaces of the PAC-T particles. Few such macropores were observed on surfaces of the S-PAC-T particles, which suggest that when S-PAC-T was produced by pulverization, fractures may have occurred at macropores, thus removing the macropores from the S-PAC surface.

3.2. *Adsorption isotherms and adsorption capacity increase*

Fig. 1 (left panel) shows adsorption isotherms for SNOM water. The amount of NOM adsorbed on S-PAC-T was about 3 times that adsorbed on PAC-T at a liquid-phase DOC concentration of 1 mg/L. The difference between the amounts of NOM adsorbed on S-PAC and PAC slightly decreased as the DOC concentration decreased, but the S-PAC-T adsorbed 2.3 times as much NOM as PAC-T at a DOC concentration of 0.4 mg/L. To clarify the reason for the larger NOM adsorption capacity of S-PAC, we evaluated the adsorption of PSSs and PEGs, which are homogeneous compounds with defined structure and molecular size similar to that of NOM. The amount of PSS-4600 adsorbed on S-PAC was 5–12 times as much as that adsorbed on PAC (Fig. 1, right panel), and the amount of PSS-1800 was 3–5 times as high (Fig. 3S of the supplementary information). There was a slight possibility that the adsorption capacity increase observed for NOM and PSS might have been an artifact of non-attainment of adsorption equilibrium; that is, the PAC–water contact times of 3 and 4 weeks used in our batch adsorption equilibrium tests might not have been sufficient for the attainment of adsorption equilibrium. Because the saturation rate for large particles is lower than that for small particles, particularly for large adsorbates, the difference in the amount of adsorbed PSS may have been due entirely to differences in the degree of equilibrium attained, even after 4 weeks of contact time. That is, the adsorption capacity we observed for PAC might have been lower than the actual value (and lower than the value for S-PAC), owing to the slower saturation rate. This possibility has been discussed in connection with experiments in which activated carbon with particle diameters of 44 μm–2.38 mm was used in 20-day adsorption tests (Randtke and Snoeyink, 1983) and experiments in which activated carbon with particle diameters of 104–750 μm was used in 2-week adsorption tests (Weber et al., 1983). However, because the activated carbon particles we used were much smaller than the particles used in these previous studies, the capacity difference was not likely to have been due to a failure to reach equilibrium. Although the amounts of adsorbed PSS-4600 observed at 1 and 2 weeks of contact time were slightly lower than the amounts at 3 weeks, the difference between the amounts at 3 and 4 weeks was very small (Fig. 1, right panel). Therefore, although some adsorption capacity may have remained after 3 weeks, that capacity was not sufficient to explain the one-order-of-magnitude difference between the isotherms of S-PAC and PAC.

We also conducted SNOM adsorption isotherm tests for other types of activated carbon including those derived from materials other than wood. The ratios of the adsorption

Table 3 – Carbon particle sizes.

S-PAC	Median diameter (μm)	Effective diameter (μm)	PAC	Median diameter (μm)	Effective diameter (μm)
S-PAC-T	0.73	0.27	PAC-T	11.8	3.9
S-PAC-W	0.66	0.23	PAC-W	6.8	2.3
S-PAC-M	0.68	0.22	PAC-M	14.3	4.2
S-PAC-F	0.67	0.23	PAC-F	26.5	5.0
S-PAC-S	0.65	0.23	PAC-S	19.1	4.3
S-PAC-D	0.67	0.23	PAC-D	8.8	2.5

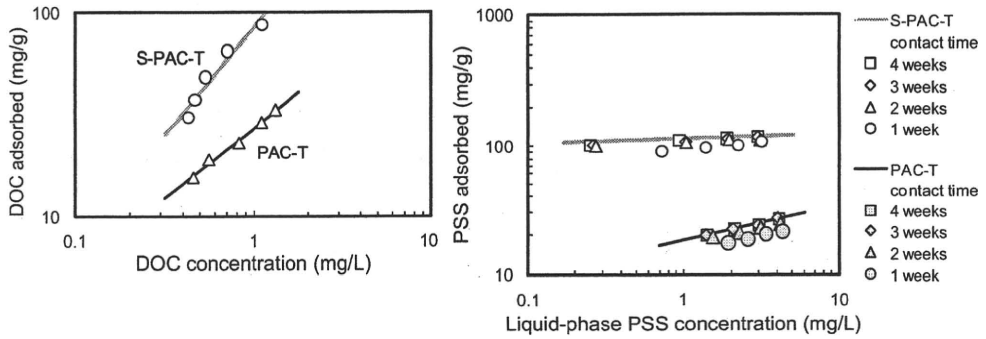

Fig. 1 – Adsorption isotherms for SNOM water (left panel) and PSS-4600 water (right panel) on S-PAC-T and PAC-T. Contact times are 3 weeks for SNOM water and 1-4 weeks for PSS-4600 water.

capacities of S-PAC and PAC ($q_{S\text{-}PAC}/q_{PAC}$) are shown in Fig. 2; $q_{S\text{-}PAC}$ and q_{PAC} were qualified as the amount of adsorbed on activated carbon in equilibrium with the liquid-phase concentration, which was equal to one-half of the initial concentration of the adsorption experiment (Table 1). For all types of carbons tested, the adsorption capacity of the S-PAC was higher than that of the corresponding PAC, although the magnitude of the increase depended on the type of carbon. Overall, the data indicate that the adsorption capacity increase was not unique to S-PAC-T.

Previous studies indicate that changes in the adsorption characteristics of activated carbon with particle size may be due to the fact that the inner regions of large particles are less accessible to the activation process during manufacturing than are the inner regions of smaller particles (Randtke and Snoeyink, 1983). Therefore, the fine fraction of activated carbon obtained by sieving might have a higher adsorption capacity than other fractions. In other words, if the outer regions of carbon particles are more active than the inner regions, partial pulverization followed by sieving to exclude the unground particle cores might lead to increased adsorption capacity. However, in this study, PAC was pulverized, but the pulverized material was not sieved. Therefore, we suspect

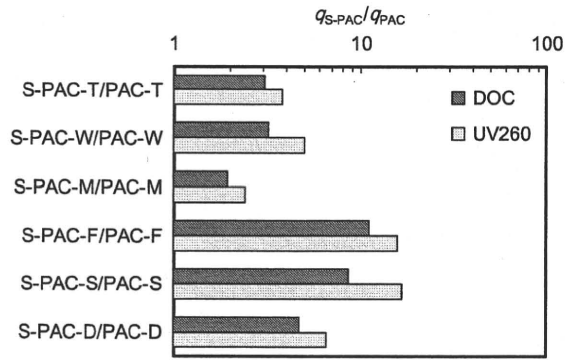

Fig. 2 – Comparison of SNOM adsorption capacity ratios for S-PAC ($q_{S\text{-}PAC}$) and PAC (q_{PAC}). $q_{S\text{-}PAC}$ and q_{PAC} were qualified as the amount of SNOM adsorbed on activated carbon in equilibrium with the liquid-phase concentration, which was equal to the half of the initial concentration of the adsorption experiment.

that the reduction of the size of the activated carbon particles due to the pulverization increased the adsorption capacity for NOM and PSS.

In contrast, the adsorption capacities of S-PAC and PAC for PEGs, in particular low-MW PEGs, did not differ substantially (Fig. 3). A slight increase in the adsorption capacity was observed for PEG-8000 (MW 8.0 kDa); however, the increase was smaller for PEG-3000, and no change was observed for PEG-1500 and PEG-300. We reported previously that the adsorption capacities of S-PAC and PAC for smaller molecules, phenol and geosmin, do not differ substantially (Matsui et al., 2004, 2009). Other researchers have reported that for low-MW pure chemicals, the adsorption capacity of activated carbon does not depend strongly on particle size (Najm et al., 1990; Letterman et al., 1974; Peel and Benedek, 1980; Leenheer, 2007). The particle diameter range used for those experiments was 14–106 μm. With respect to the PEGs, our results are in agreement with the literature results. However, it is interesting that the adsorption capacity for PEG-8000 was not markedly increased by pulverization of PAC, even though PEG-8000 has a higher MW than PSS-4600 and PSS-1800, for which the adsorption capacities were substantially increased by the particle size reduction.

3.3. *Pore size distribution*

To clarify the mechanism of the change in adsorption capacity, we obtained nitrogen adsorption data and analyzed the pore size distribution. We did not, however, obtain any clear data indicating differences between S-PAC-T and PAC-T (Fig. 4). No significant difference in pore volume or surface area in the mesopores was observed by means of the DH method, and the DFT method showed no difference in the micropores. Although S-PAC-T had a slight larger total pore volume and total pore surface than PAC-T (as indicated by the DH method), the difference was not so large when compared with the adsorption capacity differences observed for the NOMs and the PSSs. In previous work, we found that S-PAC has a higher mesopore volume than PAC, as indicated by nitrogen adsorption data and mercury porosimetry data (Matsui et al., 2004). However, when we attempted to verify this observation by measuring the pore sizes of additional samples, we observed the opposite results: that is, that PAC had slightly higher mesopore volume than S-PAC. We

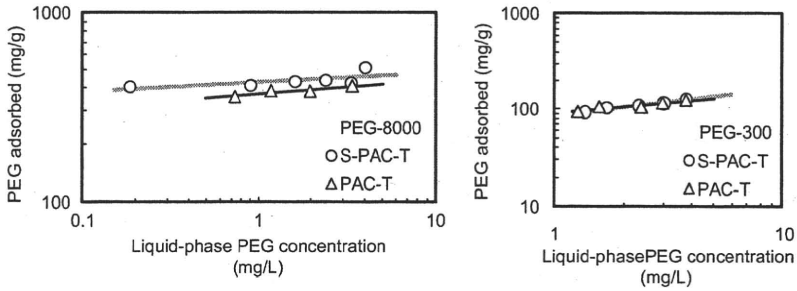

Fig. 3 – Adsorption isotherms of PEG-8000 (left panel) and PEG-300 (right panel) on S-PAC-T and PAC-T.

hypothesize that this inconsistency in the pore size change was an artifact due to a slight heterogeneity of the PAC samples we used. Therefore, in the current study, we mixed the PAC-T sample well and then separated it into two portions. One portion was used as is, and the other was pulverized to S-PAC-T. Nitrogen adsorption data were collected twice for the PAC-T and S-PAC-T samples. The difference in pore size distribution between PAC-T and S-PAC-T was small (Fig. 4). We also measured nitrogen adsorption isotherms for two additional pairs of PAC samples: again no significant difference in pore size distribution between PAC and S-PAC was observed (data not shown). The 5-fold increase in PSS adsorption capacity could not be explained even with the pore size data of the earlier study (Matsui et al., 2004), which showed increased mesopore volume after pulverization.

Weber et al. (1983) observed high NOM adsorption capacity on small-particle-size granular activated carbon, which was obtained by grinding larger particles, and hypothesized an increase in the mesopore volume due to fracture of ink-bottle pores, which are open pores with narrow, short necks and wide, closed cavities (the narrow necks permit the entry of small molecules but not larger molecules). Before the grinding, some of the mesopores are inaccessible to large adsorbate molecules because of ink-bottle constrictions in the internal pores of the adsorbents. Pulverization introduces fractures at constrictions in the ink-bottle structures so as make the interior pores accessible to large adsorbate molecules. If ink-bottle pore structures are present, nitrogen desorption methods overestimate the volume of the small pores and underestimate the volume of large pores because the size of the interior pores beyond the constriction are falsely regarded as being the size of the constriction (Adamson and Klerer, 1990). As a result, such interior pores seem to be larger after fracturing than before, and this phenomenon effectively increases the total volume of larger pores. On the

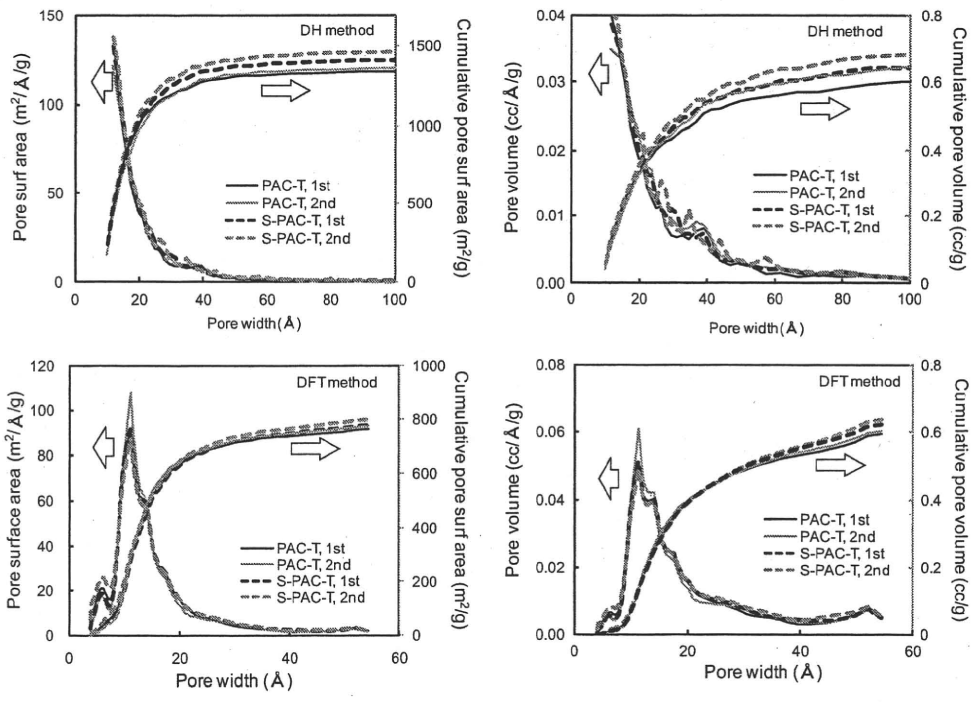

Fig. 4 – Pore size distributions of S-PAC-T and PAC-T. The designations "1st" and "2nd" refer to the two data sets obtained for each sample portion.

basis of this ink-bottle fracture hypothesis, we would expect to see a decrease in the micropore volume and an increase in mesopore volume after pulverization in our study. In Fig. 4, however, no such decrease was clearly observed by means of the DH or DFT method. Fig. 4S (supplementary information) shows the nitrogen adsorption/desorption isotherms for S-PAC and PAC. There was no distinct hysteresis loop attributable to ink-bottle structures with reference to the International Union of Pure and Applied Chemistry classification of adsorption hysteresis (Kaneko, 1994). Both PAC and S-PAC showed similar hysteresis behavior, and this type of hysteresis behavior is often observed for microporous carbon with mesopores. It is, therefore, unlikely that the structural features of internal pores were greatly changed by pulverization.

3.4. *Possible mechanisms for the increase in NOM adsorption*

Adsorption isotherms were obtained for 14 adsorbates of different characteristics. The effect of particle size on adsorption capacity was quantified in terms of $q_{S\text{-}PAC}/q_{PAC}$. An increase in adsorption capacity was observed for the PSSs, and $q_{S\text{-}PAC}/q_{PAC}$ increased as the MW of the PSS increased (Fig. 5). The ratios for the PEGs were markedly smaller than those for the PSSs. The results for the various NOM samples are shown in Fig. 6; the NOM samples are listed in the order of decreasing weight-average MW (Yau et al., 1979) and SUVA value because these are major indices for characterizing NOM (Tambo and Kamei, 1980; Tambo et al., 1989; Edzwald, 1993). SHA, which had the highest MW, showed the highest $q_{S\text{-}PAC}/q_{PAC}$ value, and post-coagulation water, which had the lowest MW, showed the lowest $q_{S\text{-}PAC}/q_{PAC}$ value. In contrast to the PSS results, the NOM results showed no clear correlation between $q_{S\text{-}PAC}/q_{PAC}$ and MW. However, NOM samples with higher SUVA values (meaning more chromophoric NOM, which has larger amount of aromatic and conjugated double bond structures) showed larger $q_{S\text{-}PAC}/q_{PAC}$ ratios. This result is in agreement with the result for PSSs and PEGs, which is consistent with the fact that PSSs have benzene rings, whereas PEGs are oligomers with no aromatic or conjugated double bonds. Salts influence NOM adsorption (Randtke and Jepsen, 1982; Weber et al., 1983). The difference in $q_{S\text{-}PAC}/q_{PAC}$ ratios shown in Fig. 6, however, cannot not be mainly attributable to the salt effect, because a larger $q_{S\text{-}PAC}/q_{PAC}$ ratio was observed for SHA than for Hakucho even though the samples were dissolved in water with the same ionic composition.

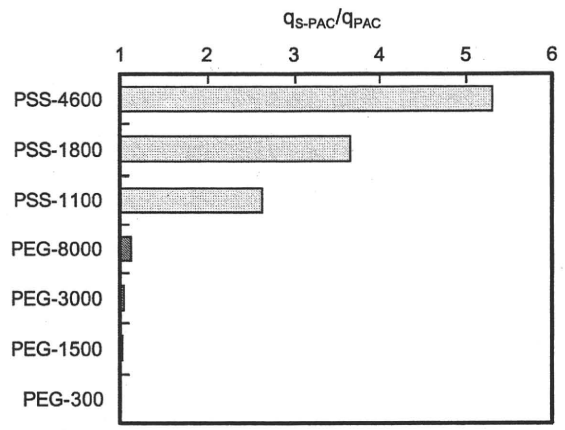

Fig. 5 – Comparison of PSS adsorption capacity ratios for S-PAC-T ($q_{S\text{-}PAC}$) and PAC-T (q_{PAC}). $q_{S\text{-}PAC}$ and q_{PAC} were qualified as the amount of PSS adsorbed on activated carbon in equilibrium with the liquid-phase concentration of 2.5 mg/L.

Because a high-SUVA value indicates high humic content (Westerhoff et al., 1999; Amy and Cho, 1999), the data shown in Fig. 6 indicate that, among the NOM types, the humic substances were more adsorbed on S-PAC than on PAC. Adsorption of humic substances on activated carbon is increased by increasing ionic strength, increasing divalent metal concentration, or decreasing solution pH (Summers and Roberts, 1988; Randtke and Jepsen, 1982; Weber et al., 1983). Although increases in capacity are partly a result of physical reduction in macromolecule size, which occurs in solution prior to adsorption, neutralization of charge on humic acid molecules in the adsorbed state may also be important (Kilduff et al., 1996b). Enhanced NOM adsorption in the presence of calcium is explained by the neutralization of electrostatic repulsion between the adsorbate and the adsorbent and by formation of an adsorbent–salt–adsorbate complex (Frederick and Cannon, 2001, a more detailed mechanism is described by Newcombe and Drikas, 1997, and Bjelopavlic et al., 1999). Li et al. (2002) also reported that the effect of Ca (II) depends on the source of the NOM. The adsorption capacity for a commercial humic acid increases with increasing Ca(II) concentration, whereas the adsorption capacity for a natural river water NOM is much less affected, and that for NOM remaining after aluminum-coagulation and filtration is unaffected. The SUVA values of the tested water in the experiment of Li et al. are 7.7 for the commercial humic acid, 2.15 for the river water, and 1.51 L/(mg·m) for the NOM remaining after aluminum-coagulation and filtration (these values were not mentioned by Li et al.). These values indicate that the effect of Ca(II) is observed for high-SUVA NOM (that is, the humic substances) but not for low-SUVA NOM. In our experiment, the increase in NOM adsorption capacity due to pulverization was prominently observed for high-SUVA NOM but not for low-SUVA NOM. Therefore, we suspected that the increase in NOM adsorption capacity resulting from pulverization might be related to Ca(II) concentration; thus, we conducted adsorption experiments of SNOM in three ionic solutions: Solution-Na (containing Na), Solution-K (K + Na), and Solution-Ca (Ca + Na). The concentrations of all cations were 1.3 meq/L (see Table 2). Fig. 7 shows the $q_{S\text{-}PAC}/q_{PAC}$ ratios for the three solutions. The presence of Ca(II) in solution increased the $q_{S\text{-}PAC}/q_{PAC}$ ratio indicating the enhanced the adsorption on S-PAC compared with PAC. However, $q_{S\text{-}PAC}$ was larger than q_{PAC} though the solution contained no Ca(II). Therefore, the presence of cations, in particular multivalent cations such as Ca(II), might have been related to the increased adsorption capacity of S-PAC for high-SUVA NOM.

Humic substances are regarded as molecular associations of relatively small molecules held together by weak interaction forces (Clapp and Hayes, 1999). The association is controlled by the

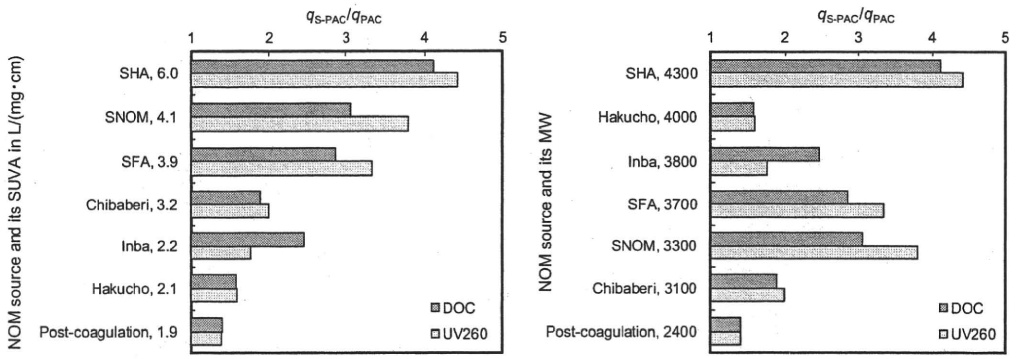

Fig. 6 – Comparison of NOM adsorption capacity ratios for S-PAC-T ($q_{S\text{-}PAC}$) and PAC-T (q_{PAC}). $q_{S\text{-}PAC}$ and q_{PAC} were qualified as the amount of NOM adsorbed on activated carbon in equilibrium with the liquid-phase concentration, which was equal to the half of the initial concentration of the adsorption experiment.

solution pH and the presence of cations, in particular, multivalent cations including Ca(II). Measurements of molecular diffusivity and membrane mass transfer suggest that the increases in ionic strength cause a reduction of molecular size in solution (Cornel et al., 1986; Kilduff and Weber, 1992). By using photon correlation spectroscopy, however, Baalousha et al. (2006) recently showed that increasing the Ca(II) concentration leads to SHA aggregation. In their experiment, however, the average size of SHA aggregates was measured at Ca(II) concentrations of 1, 10, 50, and 100 mM. Therefore, it is not clear from their data whether the aggregation of SHA occurs at a Ca(II) concentration of less than 1 mM, the concentration at which our experiments were conducted.

Because the surfaces of the activated carbons were negatively charged (zeta potential values of S-PAC-T ranged from −22 to −36 mV at pH 7 and 0.7–1.9-mmol/L ionic strength, similar to those of the SHA adsorption experiments), cations (particular multivalent cations) may accumulate from the bulk solution, and this accumulation might lead to high concentrations of cations including Ca(II) in the activated carbon pores. To confirm this, we determined the calcium mass balance for the Ca(II)-activated carbon system (in the absence of NOM so we could exclude the effect of any formation of a NOM–Ca(II) complex) and estimated the Ca concentrations in the activated carbon pores from the mass balance equation (a detailed explanation of the experimental and calculation procedures is in the supplementary information). As shown in Fig. 8, the overall Ca(II) concentrations (the amount of Ca in the pore divided by pore volume) were 23 mM for S-PAC and 12.5 mM for PAC. These concentrations were high enough for the aggregation of SHA according to the results of Baalousha et al. (2006). If adsorbates could form aggregates as a result of the cation concentrated in the activated carbon pores, aggregation may have started to occur as the NOM entered the pores, and the aggregation may have enhanced the accumulation of NOM. Aggregated NOM cannot diffuse further into the activated carbon particles once it has aggregated, so NOM may have accumulated in the vicinity of the outer surface of the carbon particles. NOM therefore may be able to penetrate activated carbon only a certain distance from the external surface, regardless of the size of the activated carbon particle. Therefore, a larger fraction of the internal pore volume is accessible with carbon of smaller particle size. According to this hypothesis, the maximum amount of NOM adsorbed should depend on the total external particle surface area of the adsorbent exposed to bulk solution. Therefore, S-PAC, which has a much larger specific external surface area per unit mass, could adsorb more NOM and PSS than could PAC.

The results shown in Fig. 2 and Table 3, however, suggest that change in particle size alone does not explain the

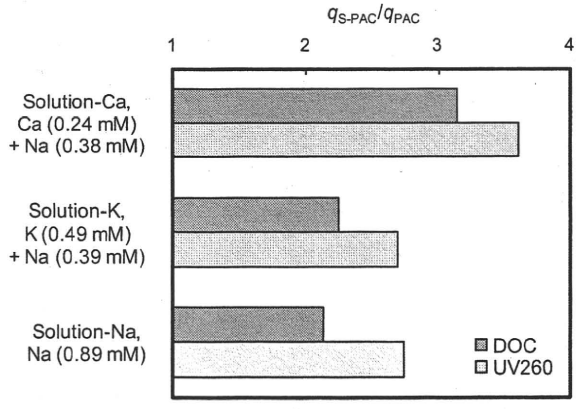

Fig. 7 – Comparison of SNOM adsorption capacity ratios for S-PAC-T (qS-PAC) and PAC-T (qPAC): effect of cations. Cation concentrations = 0.5 meq/L, pH = 7.0 ± 0.1, and alkalinity = 20 mg/L.

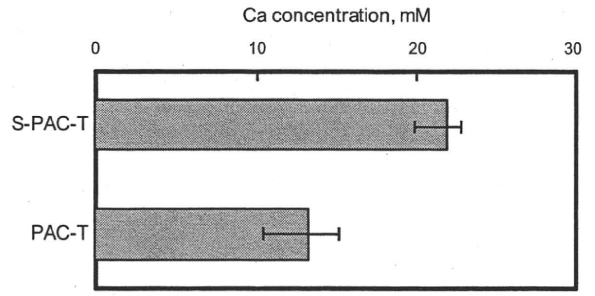

Fig. 8 – Estimated Ca(II) concentration in internal pores of S-PAC-T and PAC-T particles (error bars indicate maximum and minimum values for the 5 experiments).

increase in the capacity. Comparison of the changes in the effective diameters of PACs with respect to the corresponding S-PAC suggests that the largest changes occurred for PACs M, F, and S. Although the capacity increase was highest for PACs F and S, it was the lowest for PAC M (Fig. 2). The increase in adsorption capacity can be explained by the preferential adsorption near the outer surface of the particle (little penetration into the adsorbent particle), but the extent of this preferential adsorption may be changed by surface chemistry or pore structure of the adsorbent.

4. Conclusions

S-PACs, which have particle sizes in the submicron range and thus are much smaller than normal PAC particles, were produced by pulverization of normal PACs. The effects of particle size on the adsorption capacity for 7 NOMs (weight-average MWs from 2.4 to 4.3 kDa), 3 PSSs (MWs from 1.1 to 4.6 kDa), and 4 PEGs (MWs from 0.3 to 8 kDa) with different characteristics were investigated. The following conclusions were reached:

(1) S-PAC had a much higher (2–10 fold) adsorption capacity than PAC for the NOMs and the PSSs. This was true for two wood-based carbons, two coconut-based carbons, and one coal-based carbon. For the PEGs with MWs of 0.3 and 1.5 kDa, the adsorption capacities of S-PAC were almost the same as those of PAC. For PEGs with MWs of 3.0 and 8.0 kDa, the adsorption capacities were slightly higher for S-PAC than for PAC. Nitrogen adsorption/desorption analysis did not show a marked change in the pore size distribution, even for mesopores. Therefore, the increase in NOM and PSS adsorption capacity could not have been related to the molecular weight of the adsorbates.
(2) The ratio of the adsorption capacities of S-PAC and PAC for NOM increased as the SUVA value of the NOM increased. The ratio for PSSs increased with as the MW of the PSS increased.
(3) We hypothesize that NOM, in particular high-SUVA NOM, and PSS formed aggregates, which accumulated in the vicinity of the outer surface of the carbons particles, and thus NOM and PSS could not diffuse further into the activated carbon particles. Because NOM and PSS could preferentially adsorb near the outer surface of the adsorbent particles, the specific outer surface area (surface area per unit mass) available for adsorption would be greater for smaller adsorbent particles, and hence NOM and PSSs adsorption capacity could be larger on S-PAC, which had a much smaller particle size than PAC.

Acknowledgements

This study was supported by Grant-in-Aid for Scientific Research A (21246083) from the Ministry of Education, Culture, Sports, Science and Technology of the Government of Japan, by a research grant from the Ministry of Health, Labour and Welfare, and by Metawater Co., Tokyo, Japan. The authors thank Mr. N. Shirasaki and Mr. H. Suzuki of Hokkaido University who helped with the zeta potential analysis.

Appendix. Supplementary information

Additional details, including Figs. 1S–4S and the experimental and calculation procedures for Fig. 8, are available in the online version at doi:10.1016/j.watres.2010.05.029.

REFERENCES

Adamson, A.W., Klerer, J., 1990. Physical Chemistry of Surfaces. John Wiley & Sons. 1990.
Amy, G., Cho, J., 1999. Interactions between natural organic matter (NOM) and membranes: rejection and fouling. Water Science and Technology 40 (9), 131–139.
Baalousha, M., Motelica-Heino, M., Coustumer, P.L., 2006. Conformation and size of humic substances: effects of major cation concentration and type, pH, salinity, and residence time. Colloids and Surfaces A: Physicochemical and Engineering Aspects 272 (1–2), 48–55.
Bjelopavlic, M., Newcombe, G., Hayes, R., 1999. Adsorption of NOM onto activated carbon: effect of surface charge, ionic strength, and pore volume distribution. Journal of Colloid and Interface Science 210 (2), 271–280.
Chang, C.F., Chang, C.Y., Höll, W., Ulmer, M., Chen, Y.H., Groβ, H. J., 2004. Adsorption kinetics of polyethylene glycol from aqueous solution onto activated carbon. Water Research 38 (10), 2559–2570.
Chin, Y.P., Gschwend, P.M., 1991. The abundance, distribution, and configuration of porewater organic colloids in recent sediments. Geochimica et Cosmochimica Acta 55 (5), 1309–1317.
Clapp, C.E., Hayes, M.H.B., 1999. Sizes and shapes of humic substances. Soil Science 164 (11), 777–789.
Cornel, P.K., Summers, R.S., Roberts, P.V., 1986. Diffusion of humic acid in dilute aqueous solution. Journal of Colloid and Interface Science 110 (1), 149–164.
Edzwald, J.K., 1993. Coagulation in drinking water treatment: particles, organics, and coagulants. Water Science and Technology 27 (11), 21–35.
Frederick, H.T., Cannon, F.S., 2001. Calcium-NOM loading onto GAC. Journal of American Water Works Association 93 (12), 77–89.
Kaneko, K., 1994. Determination of pore size and pore size distribution: 1. Adsorbents and catalysts. Journal of Membrane Science 96 (1–2), 59–89.
Karanfil, T., Kilduff, J.E., Schlautman, M.A., Weber Jr., W.J., 1996a. Adsorption of organic macromolecules by granular activated carbon .1. Influence of molecular properties under anoxic solution conditions. Environmental Science and Technology 30 (7), 2187–2194.
Karanfil, T., Schlautman, M.A., Kilduff, J.E., Weber Jr., W.J., 1996b. Adsorption of organic macromolecules by granular activated carbon .2. Influence of dissolved oxygen. Environmental Science and Technology 30 (7), 2195–2201.
Kilduff, J.E., Weber Jr., W.J., 1992. Transport and separation of organic macromolecules in ultrafiltration processes. Environmental Science and Technology 26 (3), 569–577.

Kilduff, J.E., Karanfil, T., Chin, Y.P., Weber Jr., W.J., 1996a. Adsorption of natural organic polyelectrolytes by activated carbon: a size-exclusion chromatography study. Environmental Science and Technology 30 (4), 1336–1343.

Kilduff, J.E., Karanfil, T., Weber Jr., W.J., 1996b. Competitive interactions among components of humic acids in granular activated carbon adsorption systems: effects of solution chemistry. Environmental Science and Technology 30 (4), 1344–1351.

Leenheer, J.A., 2007. Progression from model structures to molecular structures of natural organic matter components. Annals of Environmental Science 1, 57–68.

Letterman, R.D., Quon, J.E., Gemmell, R.S., 1974. Film transport coefficient in agitated suspensions of activated carbon. Journal of Water Pollution Control Federation 46 (11), 2536–2547.

Li, F., Yuasa, A., Ebie, K., Azuma, Y., Hagishita, T., Matsui, Y., 2002. Factors affecting the adsorption capacity of dissolved organic matter onto activated carbon: modified isotherm analysis. Water Research 36 (18), 4592–4604.

Li, Q., Snoeyink, V.L., Mariãas, B.J., Campos, C., 2003a. Elucidating competitive adsorption mechanisms of atrazine and NOM using model compounds. Water Research 37 (4), 773–784.

Li, Q., Snoeyink, V.L., Mariñas, B.J., Campos, C., 2003b. Three-component competitive adsorption model for flow-through PAC systems. 1. Model development and verification with a PAC/membrane system. Environmental Science and Technology 37 (13), 2997–3004.

Matsui, Y., Fukuda, Y., Murase, R., Aoki, N., Mima, S., Inoue, T., Matsushita, T., 2004. Micro-ground powdered activated carbon for effective removal of natural organic matter during water treatment. Water Science and Technology: Water Supply 4 (4), 155–163.

Matsui, Y., Murase, R., Sanogawa, T., Aoki, N., Mima, S., Inoue, T., Matsushita, T., 2005. Rapid adsorption pretreatment with submicron powdered activated carbon particles before microfiltration. Water Science and Technology 51 (6–7), 249–256.

Matsui, Y., Aizawa, T., Kanda, F., Nigorikawa, N., Mima, S., Kawase, Y., 2007. Adsorptive removal of geosmin by ceramic membrane filtration with super-powdered activated carbon. Journal of Water Supply: Research and Technology-AQUA 56 (6–7), 411–418.

Matsui, Y., Ando, N., Sasaki, H., Matsushita, T., Ohno, K., 2009. Branched pore kinetic model analysis of geosmin adsorption on super-powdered activated carbon. Water Research 43 (12), 3095–3103.

Najm, I.N., Snoeyink, V.L., Suidan, M.T., Lee, C.H., Richard, Y., 1990. Effect of particle size and background natural organics on the adsorption efficiency of PAC. Journal of American Water Works Association 82 (1), 65–72.

Newcombe, G., Drikas, M., 1997. Adsorption of NOM onto activated carbon: electrostatic and non-electrostatic effects. Carbon 35 (9), 1239–1250.

Peel, R.G., Benedek, A., 1980. Attainment of equilibrium in activated carbon isotherm studies. Environmental Science and Technology 14 (1), 66–71.

Randtke, S.J., Jepsen, C.P., 1982. Effects of salts on activated carbon adsorption of fulvic acid. Journal of American Water Works Association 74 (2), 84–93.

Randtke, S.J., Snoeyink, V.L., 1983. Evaluating GAC adsorptive capacity. Journal of American Water Works Association 75 (8), 406–413.

Summers, R.S., Roberts, P.V., 1988. Activated carbon adsorption of humic substances. II. Size exclusion and electrostatic interactions. Journal of Colloid and Interface Science 122 (2), 382–397.

Tambo, N., Kamei, T., 1980. Water quality conversion matrix of aerobic biological processes. Journal of Water Pollution Control Federation 52 (5), 1019–1028.

Tambo, N., Kamei, T., Itoh, H., 1989. Evaluation of extent of humic-substance removal by coagulation. In: Suffet, I.H., MacCarthy, P. (Eds.), Aquatic Humic Substances: Influence on Fate and Treatment of Pollutants. American Chemical Society, Washington DC, pp. 453–471.

Tanaka, H., Matsui, Y., Ohno, K., Itoh, M., Ueki, M., Yoshizawa, K., Kobayashi, T., Miki, K., Aoi, K. Okazaki, M. (2008) A study on water treatment by using nanofiltration membrane (III). Proceedings of the Annual Conference of Japan Water Works Association, pp. 208–209. Sendai, Japan (in Japanese).

Weber Jr., W.J., Voice, T.C., Jodellah, A., 1983. Adsorption of humic substances: the effects of heterogeneity and system characteristics. Journal of American Water Works Association 75 (12), 612–619.

Westerhoff, P., Aiken, G., Amy, G., Debroux, J., 1999. Relationships between the structure of natural organic matter and its reactivity towards molecular ozone and hydroxyl radicals. Water Research 33 (10), 2265–2276.

Yau, W.W., Kirkland, J.J., Bly, D.D., 1979. Modern Size Exclusion Chromatography. Wiley Interscience, New York.